2010

Total Solar Eclipse Observations of Hot Prominence Shrouds

Shadia Rifai Habbal
University of Hawaii

Miloslav Druckmüller
Technical University of Brno

Huw Morgan
University of Hawaii

I. Scholl
University of Hawaii

V. Rusin
Astronomical Institute, Slovak Academy of Sciences

See next page for additional authors

Authors
Shadia Rifai Habbal, Miloslav Druckmüller, Huw Morgan, I. Scholl, V. Rusin, Adrian Daw, Judd Johnson, and Martina B. Arndt

The Astrophysical Journal, 719:1362–1369, 2010 August 20 doi:10.1088/0004-637X/719/2/1362

TOTAL SOLAR ECLIPSE OBSERVATIONS OF HOT PROMINENCE SHROUDS

S. Rifai Habbal[1], M. Druckmüller[2], H. Morgan[1], I. Scholl[1], V. Rušin[3], A. Daw[4,5], J. Johnson[6], and M. Arndt[7]
[1] Institute for Astronomy, University of Hawaii, 2680 Woodlawn Drive, Honolulu, HI 96822, USA; shadia@ifa.hawaii.edu
[2] Faculty of Mechanical Engineering, Brno University of Technology, 616 69 Brno, Czech Republic
[3] Astronomical Institute, Slovak Academy of Sciences, 059 60 Tatranska Lomnica, Slovakia
[4] Department of Physics and Astronomy, Appalachian State University, 525 Rivers Street, Boone, NC 28608, USA
[5] NASA Goddard Space Flight Center, Greenbelt, MD, USA
[6] Electricon, Boulder, CO 80204, USA
[7] Physics Department, Bridgewater State College, Conant Science Building, 24 Park Avenue, Bridgewater, MA 02325, USA
Received 2010 June 3; accepted 2010 June 26; published 2010 July 28

ABSTRACT

Using observations of the corona taken during the total solar eclipses of 2006 March 29 and 2008 August 1 in broadband white light and in narrow bandpass filters centered at Fe x 637.4 nm, Fe xi 789.2 nm, Fe xiii 1074.7 nm, and Fe xiv 530.3 nm, we show that prominences observed off the solar limb are enshrouded in hot plasmas within twisted magnetic structures. These shrouds, which are commonly referred to as cavities in the literature, are clearly distinct from the overlying arch-like structures that form the base of streamers. The existence of these hot shrouds had been predicted by model studies dating back to the early 1970s, with more recent studies implying their association with twisted magnetic flux ropes. The eclipse observations presented here, which cover a temperature range of 0.9 to 2 $\times 10^6$ K, are the first to resolve the long-standing ambiguity associated with the temperature and magnetic structure of prominence cavities.

Key words: magnetic fields – Sun: corona – Sun: filaments, prominences – Sun: magnetic topology

1. INTRODUCTION

Prominences are some of the most intriguing magnetic and density structures to appear in the solar corona during a total solar eclipse. High spatial resolution observations reveal intricate twisted threads, which extend from a few arcseconds to over 0.25 $R_\odot$ above the limb. Janssen (1868) and Secchi (1875, 1877) were the first to use the then recently invented spectrograph to unravel the mystery of their pinkish hue, which they soon discovered was produced by Hα emission. At present, ample observational evidence points to their cool temperature of a few times 10^4 K and high electron density in the range 10^9–10^{11} cm^{-3} (see, e.g., review by Engvold 1990). Their plasma properties continue to be intriguing in light of the typical ambient coronal temperatures of at least 10^6 K and densities on the order of a few times 10^8 cm^{-3}.

In eclipse and coronagraph observations, prominences are always seen lying at the base of streamers and their distribution is linked to the large-scale structure of the corona (Morgan & Habbal 2007, 2010). Their immediate surroundings are frequently characterized by reduced white light emission, which has led to the commonly used term of "prominence cavity." A system of concentric arch-like arcades is found to overlie the cavities (Saito & Tandberg-Hanssen 1973). When observed against the solar disk, prominences are called filaments, and both filaments and their associated cavities appear in absorption rather than emission. Except for Hα observations, they are indistinguishable in coronal emission lines, such as in the extreme ultraviolet and in X-rays. The presence of these cavities has been the subject of numerous investigations (see, e.g., comprehensive reviews by Tandberg-Hanssen 1995; Mackay et al. 2010, and references therein). Despite extensive observations, at present little is known about their thermodynamic properties.

In one of the earlier models of the thermodynamic structure of prominences and their associated cavities, Pneuman (1972, p. 803) concluded "that the hottest part of a coronal helmet could be the coronal cavity." Pneuman reported that supporting evidence was provided from eclipse observations of the Fe xiv line during the 1970 March 7 eclipse (in private communication from J. T. Gosling and R. A. Kopp cited in Pneuman 1972). More recently, Hudson et al. (1999) provided observations of soft X-ray emission overlapping a prominence core and cavity along the line of sight aligned with the axis of a prominence observed off the limb. In an attempt to model these soft X-ray observations, Fan & Gibson (2006) proposed that "bright cores" in a filament channel could be the signature of a boundary layer or current sheet separating the helical field of a twisted flux rope, representing the prominence, from its surrounding untwisted fields. Fuller et al. (2008) modeled the cavity as a density depleted torus around the Sun and concluded that the cavity temperature derived from the assumption of hydrostatic equilibrium was around 2 $\times$ 10^6 K. In a recent study, Vásquez et al. (2009) derived the differential emission measure (DEM) curve from a tomographic reconstruction of observations of prominences made off the limb with the *STEREO* spacecraft in the extreme ultraviolet. The peak of the DEM was around 2 $\times$ 10^6 K, which they concluded was likely to be the temperature of the prominence cavity. Hence, it seems at present that a number of model studies lead to the conclusion that hot material must be filling the so-called prominence cavities. On the other hand, the observational evidence for these hot cavities remains very limited.

Here we report on the first multiwavelength observations of prominence cavities from which their temperature is derived. These observations were made during the total solar eclipses of 2006 March 29 and 2008 August 1, as briefly described in Section 2. The high spatial resolution and radial extent of these eclipse observations, spanning the solar surface out to at least 2 $R_\odot$, are one of their main advantages. Following the analysis of the observations in Section 3, we conclude in Section 4 with the implications of these findings for models of quiescent and eruptive prominences.

2. ECLIPSE OBSERVATIONS

The first complement of high spatial resolution white light images and images of the Fe xi 789.2 nm and Fe xiii 1074.7 nm

Figure 1. Top: the solar corona in white light during the total solar eclipse of 2008 August 1. Note the lunar surface on the eclipsed solar disk or earthshine. Bottom: overlay of emission from Fe x/Fe xi in red and Fe xiii/Fe xiv in green on the white light. Both images have been processed using the technique developed by Druckmüller (2009).

coronal emission were taken during the eclipse of 2006 March 29. These observations were repeated and complemented with imaging in Fe x 637.4 nm and Fe xiv 530.3 nm at the eclipse of 2008 August 1. The peak ionization fraction for these spectral lines occurs at a temperature of 0.94×10^6 K for Fe x, 1.16×10^6 K for Fe xi, 1.6×10^6 K for Fe xiii, and 1.8×10^6 K for Fe xiv. The details of these eclipse experiments have been described by Habbal et al. (2007a, 2007b, 2010) and Pasachoff et al. (2009). Image processing (Morgan et al. 2006; Druckmüller 2009; Druckmüller et al. 2006) played a critical role in uncovering the intricate details of the coronal structures, in white light as well as in the coronal emission lines. Shown in the example of Figure 1 are the white light (top) and composite coronal emission images superimposed on white light (bottom), taken in 2008. Application of the image processing technique described by Druckmüller (2009) reveals the finest details of coronal structures down to the spatial resolution of the white light image of 1 arcsec pixel^{-1}. The ubiquitous presence of prominences at the base of streamers, underlying myriads of arch-like structures, extending out to 0.5 $R_\odot$ above the limb, is evident in the white light image.

In the composite white light-emission line image, red corresponds to the Fe x/Fe xi emission, while the turquoise/green reflects the Fe xiii/Fe xiv emission. As recently shown by Habbal et al. (2010), the composite coronal emission line image is a proxy for the electron temperature distribution in the corona. Two features stand out: the arch-like structures, forming the bases of streamers, are characterized by emission in the hotter lines of Fe xiii and Fe xiv. The expanding corona, on the other hand, is characterized by density structures that extend away from the Sun, emitting in the cooler lines of Fe x and Fe xi.

3. THERMODYNAMIC PROPERTIES OF PROMINENCE CAVITIES

To explore the thermodynamic properties of cavities in more detail, we consider four prominence-cavity examples from the 2008 eclipse observations. These are taken from four quadrants in the images of Figure 1 and shown in Figures 2–5 (northeast, southeast, southwest, and northwest). The panels in these figures are organized as follows. The top panels are close-ups of the white light image (right) combined with the color composite of the emission line observations (left). The six panels below are close-ups of the prominences and their cavities as seen (from left to right and top to bottom) in Fe x, Fe xi, Fe xiii, and Fe xiv, respectively. These are processed using the normalizing radial graded filter, or NRGF technique, described by Morgan et al. (2006). Also shown is the NRGF-processed continuum image, obtained through a narrow bandpass filter centered at 787.9 nm, in the neighborhood of the Fe xi 789.2 nm line. The corresponding section of the high spatial resolution white light image, labeled WLproc, is also included. These close-ups are displayed in a polar coordinate system (position angle, P.A., versus radial distance with P.A. increasing counterclockwise from 0° north). Emission line and continuum intensities, normalized to their corresponding maximum, are plotted below, as a function of P.A., for three heights: 1.05, 1.15, and 1.3 $R_\odot$.

There are two different prominences in the northeast quadrant (labeled as 1 and 2 in Figure 2). The white light and emission line images reveal a complex of twisted structures compared to the more streamlined and raylike neighboring features. One is anchored at the solar surface between P.A. = 30°and 40°, while the other seems suspended or detached, as seen in detail in the WLproc panel centered at P.A. = 58° and spanning P.A. = 55°–60°, between 1.15 and 1.2 $R_\odot$. These two prominences appear to be independent. Prominence 1 is relatively stable and quiescent. Prominence 2 exhibited changes in position and shape throughout the few minutes of eclipse observations (see also Pasachoff et al. 2009), with no sign of eruption during that time. Their temperature environments, as reflected by the emission lines, are also different. There is no Fe x emission around prominence 1. It is featureless in Fe xi, while strikingly localized at P.A. = 40° and brighter than its surrounding in Fe xiii and Fe xiv. This is evident in a more quantitative manner in the plots below, at 1.05 $R_\odot$, with the marked depression in Fe x coinciding with a peak in Fe xiii and Fe xiv.

The suspended prominence 2 around P.A. = 55° extends between 1.15 and 1.25 $R_\odot$. It is clearly surrounded by cooler Fe x and Fe xi emission which extends in height beyond the prominence as seen in white light (panel WLproc). There are relative dips in the intensity plots at 1.15 $R_\odot$ around P.A. = 55° in Fe xiii (red) and Fe xiv (dashed-red) where there are relative peaks in Fe x (green) and Fe xi (dashed-green).

The normalized continuum intensity is practically flat across this streamer at all heights, with no sign of a localized depression that is the trademark of a cavity around both prominences. Note that in the continuum (black line), the streamer complex as a whole has a distinct sharp boundary at P.A. = 40° at 1.15 $R_\odot$ which moves to P.A. = 50° at 1.3 $R_\odot$.

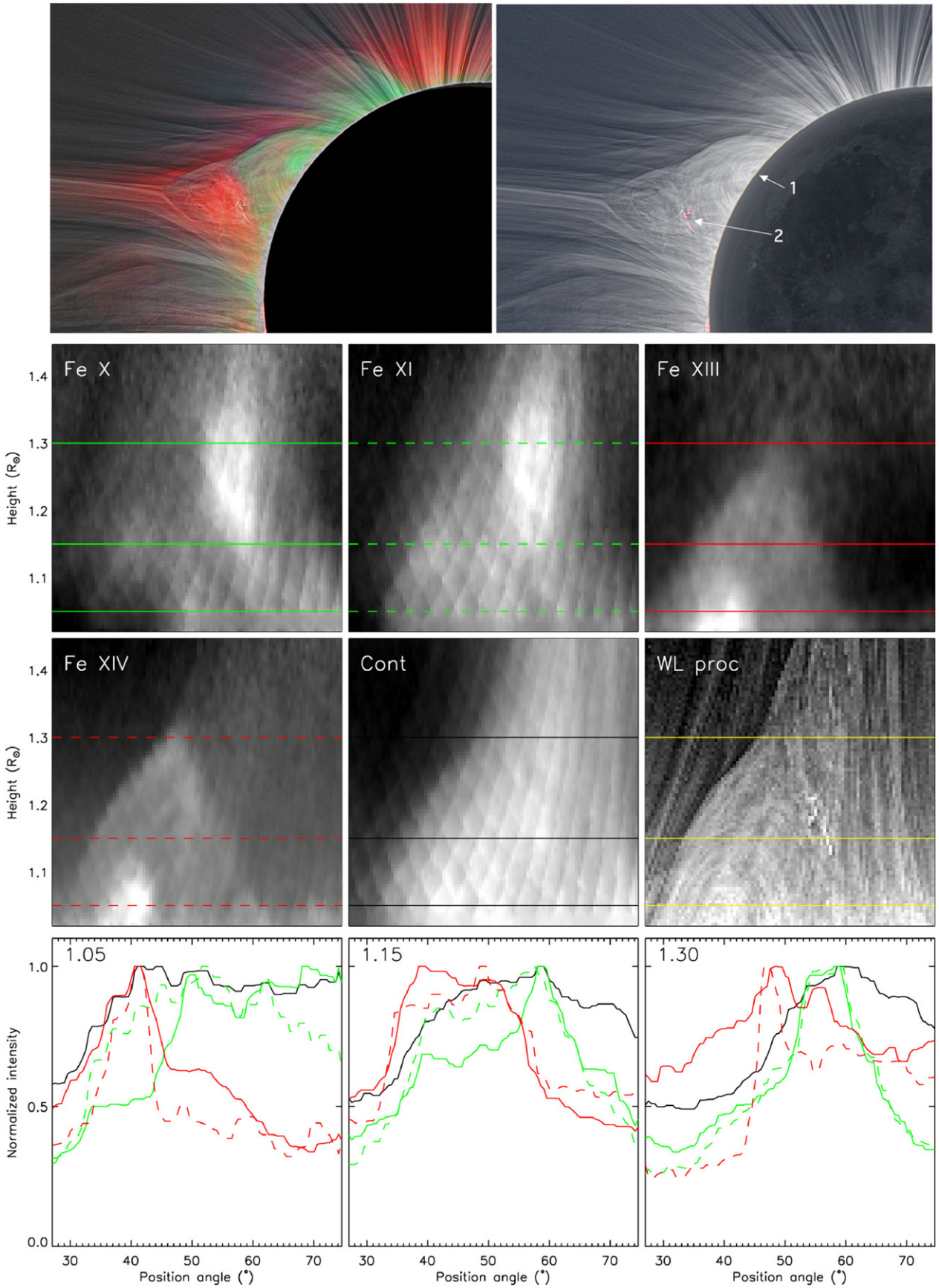

Figure 2. Top: section of the northeast quadrant of the 2008 eclipse images from Figure 1. Second and third rows: close-up views of the prominence regions in Fe X, Fe XI, Fe XIII, and Fe XIV, 787.86 nm continuum, processed with NRGF, and white light (WLproc) processed using Druckmüller's technique. Bottom row: spectral line intensities normalized to their corresponding maximum value (*y*-axis) vs. P.A. (*x*-axis), at 1.05, 1.15, and 1.3 $R_\odot$, with green = Fe X, dashed-green = Fe XI, red = Fe XIII, dashed-red = Fe XIV, and black = 787.86 nm continuum. The horizontal dashed lines correspond to the radial distances where the normalized emission line intensities are plotted.

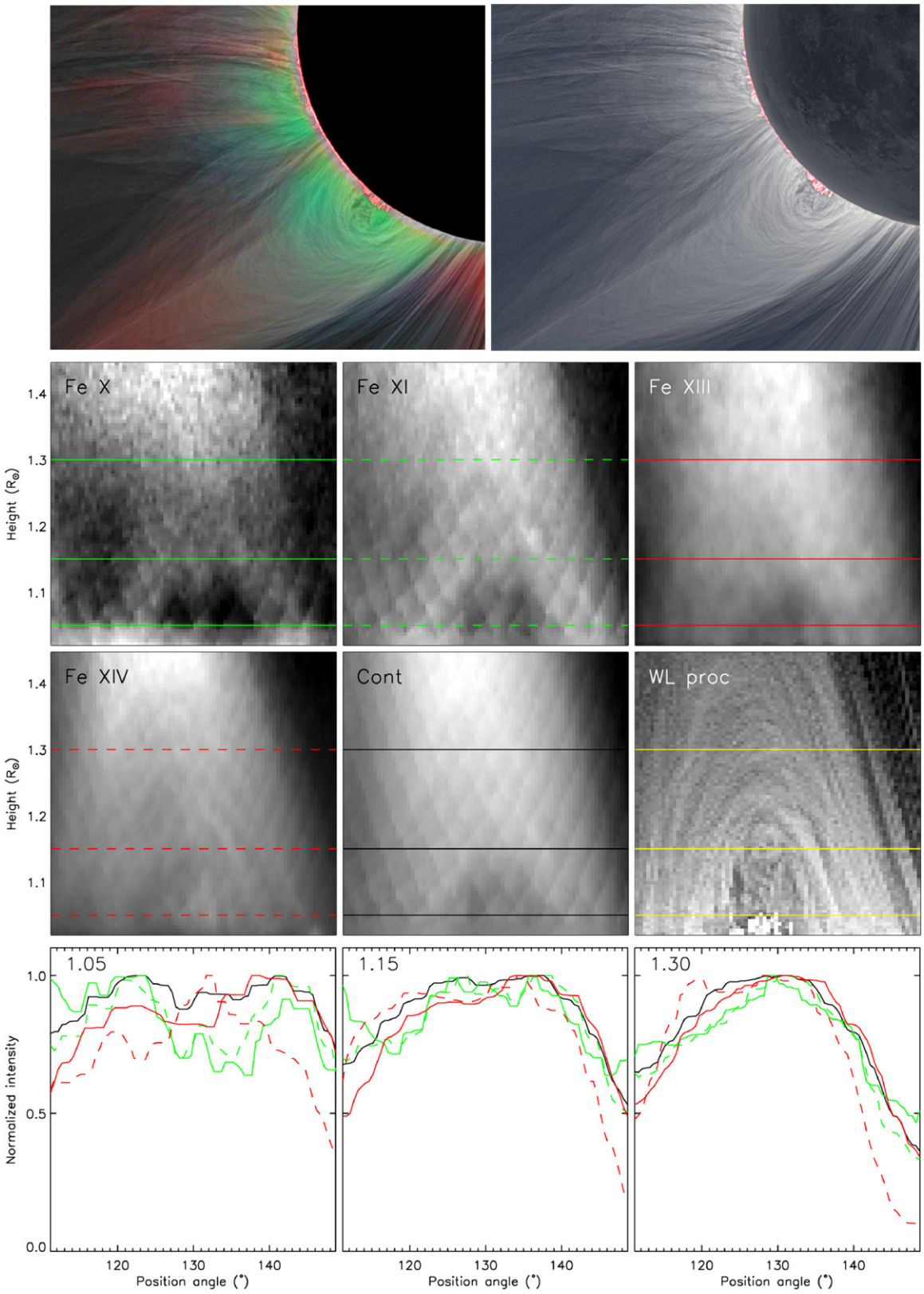

Figure 3. Same as Figure 2 but for the southeast quadrant.

In the southeast quadrant (Figure 3), a string of prominences appears as if oriented north–south along the limb. A close-up shows an intricate twisted structure, underlying a simpler arch-like configuration (see panel WLproc). This structure has a distinct double-arched cavity, which is most pronounced in the coolest lines of Fe X and Fe XI, and to some extent in Fe XIII and Fe XIV below 1.15 $R_{\odot}$. The signature of the double-arched cavity is also present in white light as seen in the black line plot in the lower panel at 1.05 $R_{\odot}$, with two minima at P.A. = 130° and 135°. This seems to be an example of a cavity that is

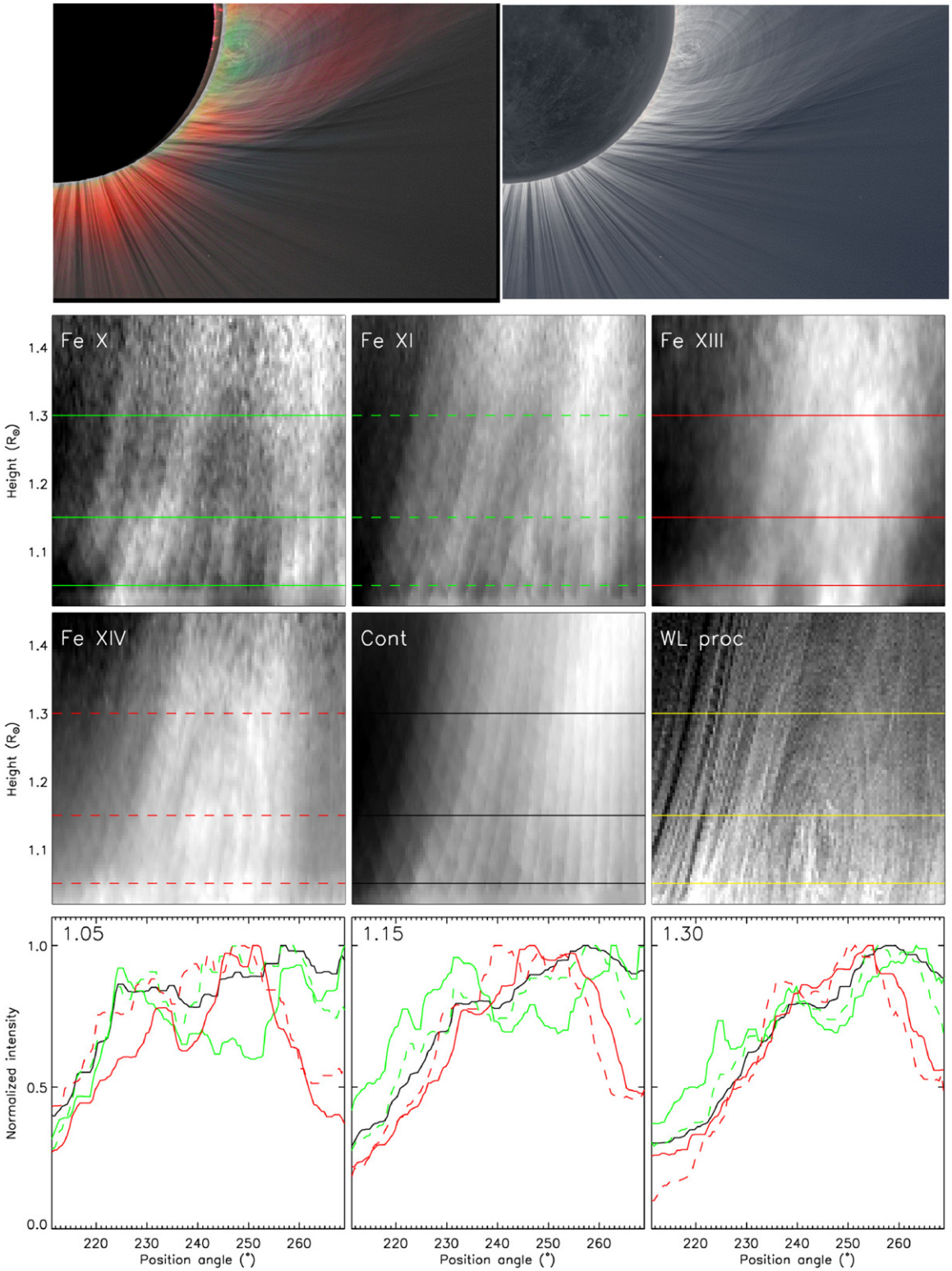

Figure 4. Same as Figure 2 but for the southwest quadrant.

probably hotter than Fe XIV as it seems to increase in brightness with increasing temperature, without quite reaching its peak at Fe XIV, the hottest temperature available in these observations.

The example of Figure 4 is that of an elongated cavity that extends out to 1.3 $R_{\odot}$, overarching the prominence, centered at P.A. = 242°. It reaches a maximum height of 1.15 $R_{\odot}$, as seen in the panel WLproc. The temperature structure of the cavity is best seen in the observed depression in the Fe X image, and to some extent in Fe XI. Part of it is seen in Fe XIII but disappears in Fe XIV. The depression is visible in the intensity plots at P.A. = 237° in Fe X and Fe XI, but in Fe X only at 250° at 1.05 $R_{\odot}$. Again at 1.15 $R_{\odot}$, both Fe X and Fe XI exhibit a depression at 240°, but only Fe X dips at 250° while Fe XI peaks at that P.A. At 1.3 $R_{\odot}$, both Fe X and Fe XI show a dip at 245°. At 1.05 and

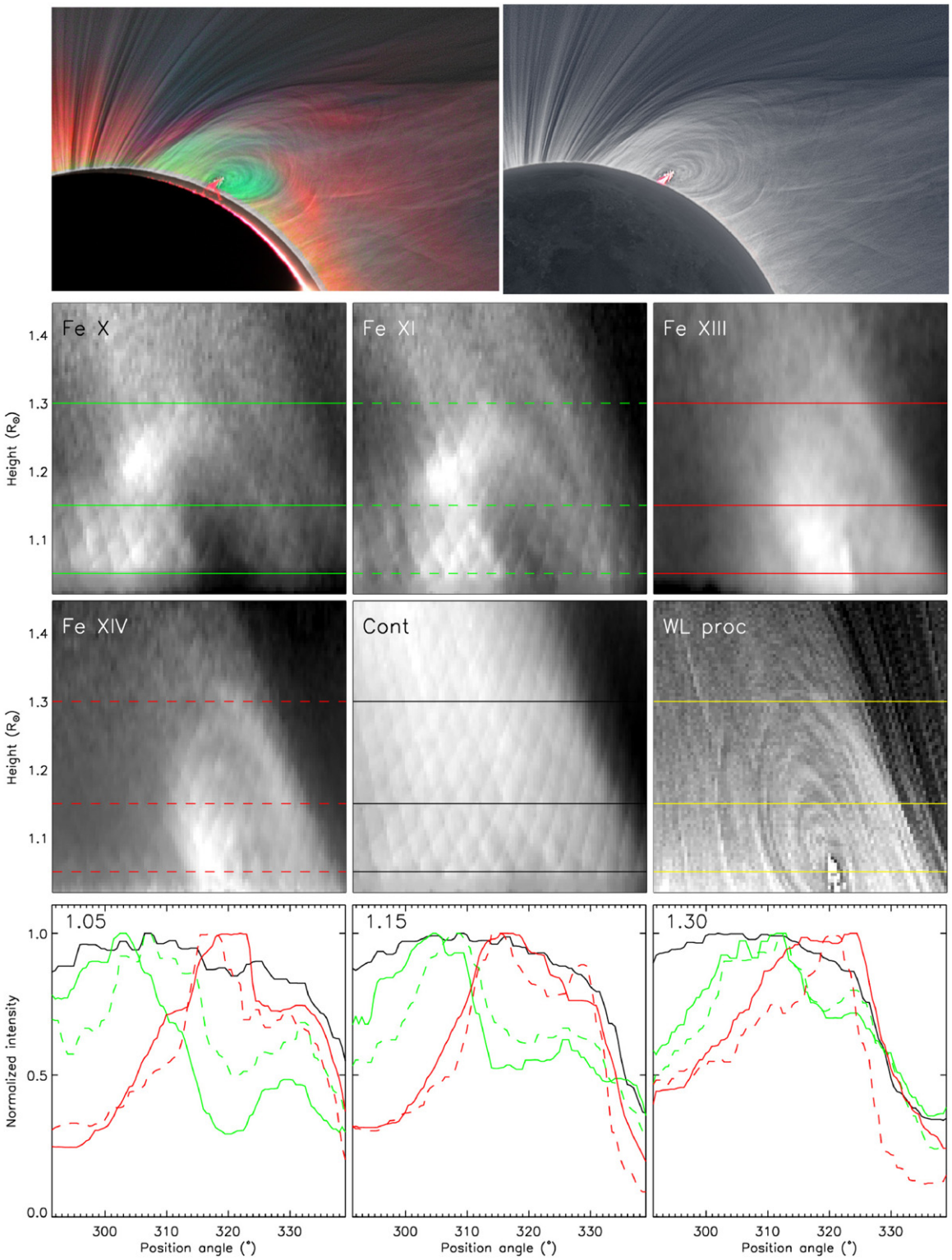

Figure 5. Same as Figure 2 but for the northwest quadrant.

1.15 $R_{\odot}$, the dips in Fe X and Fe XI are accompanied by peaks in Fe XIII with a slight offset in P.A. in Fe XIV. This example is that of a hot extended cavity, reaching a temperature of at least 2×10^6 K.

The final example pertains to a spectacular prominence located in the northwest quadrant, centered at P.A. = 320°and shown in Figure 5. The broadband white light reveals a complex structure at its base. The prominence itself is below 1.05 $R_{\odot}$. It is surrounded by a single cavity clearly distinguishable in Fe X and Fe XI, but with peaked emission in Fe XIII and Fe XIV. The cavity, however, has no signature in white light. The opposite behaviors of Fe X and Fe XI compared to Fe XIII and Fe XIV are apparent in the intensity plots, whereby the depressions centered at 320° in the former are accompanied by peaks in the latter two spectral lines at all heights.

The Sun was at its minimum of activity in 2008 compared to 2006. The observations taken during the eclipse of 2006, although not as comprehensive in wavelength coverage as in

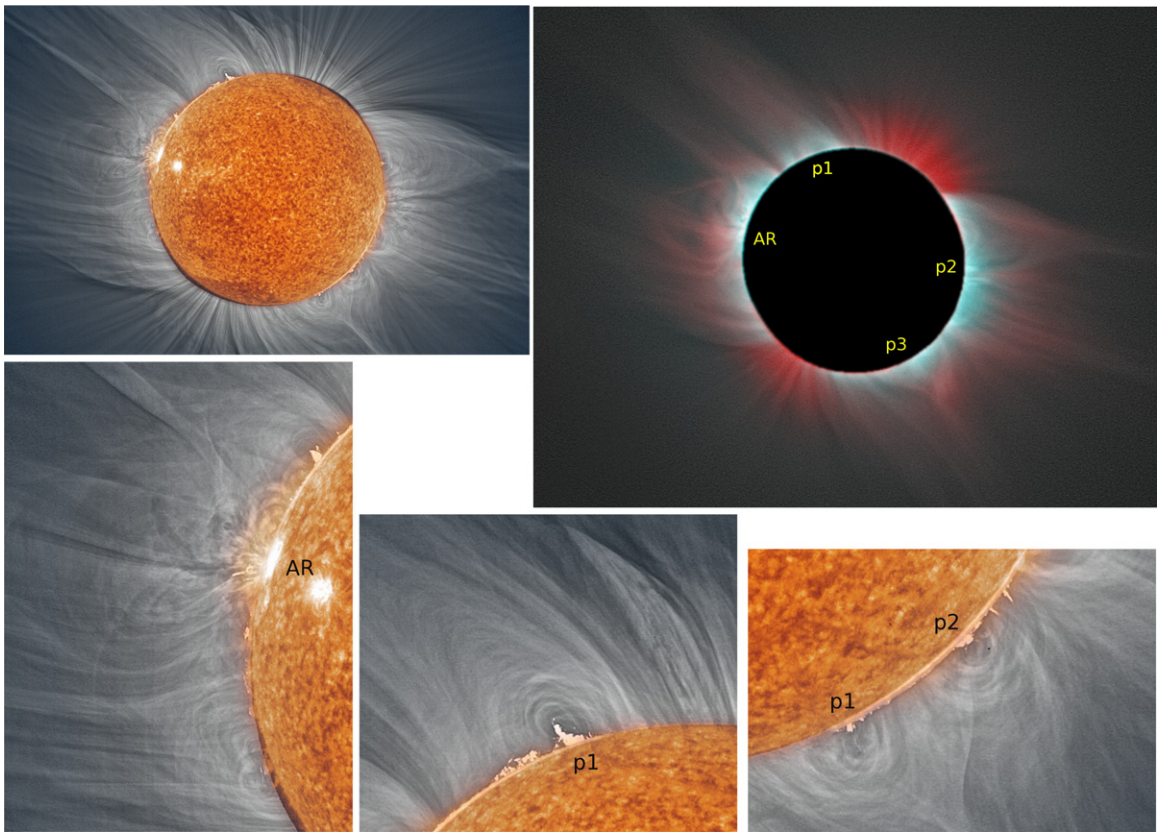

Figure 6. Top left: broadband white light image of the corona from the 2006 March 29 eclipse, processed with the Druckmüller technique. The solar disk is the EIT/*Solar and Heliospheric Observatory* (*SOHO*) He II 304 Å emission within 5 minutes of the eclipse. Top right: overlay of the white light emission and emission lines from Fe XI (red) and Fe XIII (turquoise). Lower panels, from left to right: close-up of the active region on the east limb, the northeast quadrant, and the southwest quadrant. Labels p1, p2, and p3 refer to the three largest prominences at the solar limb.

2008, offer additional supporting evidence for the findings of 2008. We limit our discussion here to the images, without going into detailed studies of individual prominence/cavity examples. Shown in Figure 6 are the exquisite details of the white light corona. Also shown in the colored figure are the Fe XI emission in red and the Fe XIII emission in blue. Details of the immediate surroundings of prominences labeled as p1, p2, and p3 are shown in the smaller panels. The advantage of the 2006 observations was the presence of an active region (labeled AR) off the limb. It is clear that the intricate density/magnetic structures observed above prominences, defining the so-called cavities, are also present over the active region complex. Here too, it is clear that the prominence cavities are mostly hot, as seen in the bluish color from Fe XIII, the hottest temperature line observed at the eclipse. Curiously, we also find that the material overlying prominences, in the so-called cavities, are hotter than the material overlying the active region complex.

Finally, we consider the orientation of the filament channels on the solar disk for the 2008 eclipse. As noted by Saito & Tandberg-Hanssen (1973), arches overlying prominences as seen projected against the sky are arcades which follow the length of a prominence. They are best seen when the orientation of a prominence, as projected against the solar disk, is predominantly east–west. The location of the filaments and their corresponding arcades, which appear as channels in projection against the solar disk, are given in the disk overlay in Figure 7. These have been reproduced from EUV/EIT images of the solar disk taken over a period of a few days preceding and following the eclipse observations, using the technique

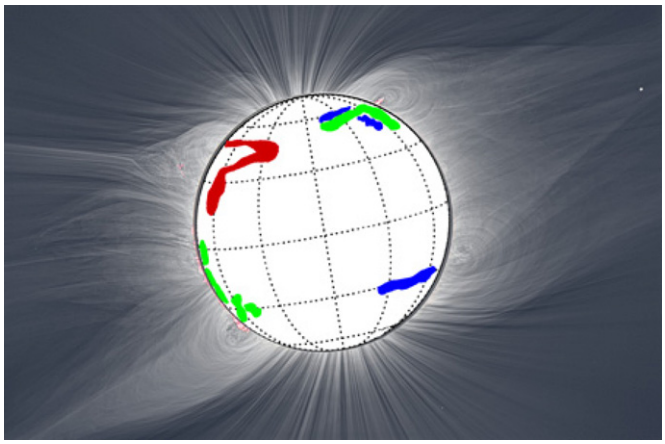

Figure 7. Overlay of filaments on the solar disk, two days before (blue), five days after (red), and the day of the 2008 August 1 eclipse (green), as derived from *SOHO* EIT Fe XI 171 Å image and *SOHO* MDI magnetograms.

described by Scholl & Habbal (2008). It is plausible that the differences in the observed environments of prominences are due in part to the orientation of their corresponding filament channels on the solar disk, from being oriented either north–south or east–west close to and at the solar limb.

4. DISCUSSION AND CONCLUSIONS

The unsurpassed quality of the 2006 and 2008 eclipse observations combining white light and emission from four

iron lines spanning temperatures from 0.9 to 2 $\times 10^6$ K, together with optimal image processing techniques, have led to a comprehensive characterization of what has been referred to in the solar physics literature as prominence or filament cavities. The two main outcomes from these observations are the realization that (1) prominence cavities are intricate magnetic/density structures, with (2) temperatures characteristic, for the most part, of 2 $\times 10^6$ plasmas or even higher. No upper limit could be placed on these values, since the hottest spectral line observed was Fe XIV.

The details of the underlying twisted and helical fine scale structures within these cavities, which are quite distinct from the rest of the surrounding structures along the line of sight, can account for the fact that cavities are not necessarily associated with depressions in white light intensity compared to their surroundings, as has been assumed in the literature so far. Clearly, the white light depressions, when observed, are a function of the orientation of the helical structures with respect to the line of sight. In general, depressions appeared in the cooler Fe X line. The example of the suspended prominence in the 2008 eclipse observations (Figure 2) was the only one where a prominence was surrounded by cool Fe X and Fe XI material.

It is also clear from these observations that the complex magnetic and density structures within the cavities are quite distinct from the magnetic structures defining the rest of the overlying arch-like structures forming the base of streamers, as well as the boundaries of streamers. The twisted and what seem observationally to be helical structures within the cavities provide the most direct evidence for the emergence of helicity with prominences that is not limited to the prominences themselves but extends to their immediate surroundings. On the other hand, the global evolution model results of Yeates et al. (2007, 2008) show that helicity associated with emerging active regions is likely to be the source of a significant (96%) fraction of the helicity in filaments, a process that may occur over a timescale of a few years. The 2008 observations were taken at the minimum of solar cycle 23 when no active regions were present for almost a year. Hence, they cannot conclusively provide supporting evidence for the helicity in prominences to be solely due to active regions.

In contrast to the relatively cool material of tens of thousands of degrees, characteristic of filaments, the helical structure of the overlying material is tenuous and hot, with temperatures exceeding two million degrees. The realization that cool and dense prominences are embedded in hot and tenuous plasmas should have significant implications for coronal heating mechanisms in the neighborhood of magnetic polarity reversal regions, since filaments are known to trace magnetic reversal lines. This conclusion had already been reached by a number of theoretical and model studies, such as by Pneuman (1972), Antiochos & Klimchuk (1991), and Fan & Gibson (2006) to name a few. The study presented here provides the first observational proof in support of these models. We further conjecture that it is precisely the interface between the twisted and complex structure of the coupled prominence-cavity material that leads to an unstable situation which triggers a coronal mass ejection. In closing, we propose that the term prominence cavity be replaced in future investigations by hot prominence shrouds, as the term "cavity" is clearly a misnomer.

Support for the eclipse observations was provided by NASA grant NNX08AQ29G and NSF grant ATM 08-02520 to the University of Hawaii, NSF grant ATM-0801633, an NC Space Grant New Investigations award to Appalachian State University (A. Daw), and NSF grant NSF-AGS-0450096 to Bridgewater State College (M. Arndt). M.D. was supported by grant 205/09/1469 from the Czech Science Foundation. V.R. was partially supported by the Slovak Academy of Sciences Grant Agency VEGA, grant 0098/10, and by the Science and Technology Assistance Agency APVT under contract APVT 51-012-704. M.D. and V.R. also acknowledge Peter Aniol's (ASTELCO) technical and financial support. We thank Dr. Duncan Mackay for his insightful comments on the emergence of helicity with active regions.

REFERENCES

Antiochos, S. K., & Klimchuk, J. A. 1991, ApJ, 378, 372
Druckmüller, M. 2009, ApJ, 706, 1605
Druckmüller, M., Rušin, V., & Minarovjech, M. 2006, Contrib. Astron. Obs. Skalnate Pleso, 36, 131
Engvold, O. 1990, in IAU Colloq. 117, Dynamics of Quiescent Prominences, ed. V. Ruzdjak & E. Tandberg-Hanssen (Berlin: Springer), 294
Fan, Y., & Gibson, S. E. 2006, ApJ, 641, L149
Fuller, J., Gibson, S. E., De Toma, G., & Fan, Y. 2008, ApJ, 678, 515
Habbal, S. R., Morgan, H., Johnson, J., Arndt, M. B., Daw, A., Jaeggli, S., Kuhn, J., & Mickey, D. 2007a, ApJ, 663, 598
Habbal, S. R., Morgan, H., Johnson, J., Arndt, M. B., Daw, A., Jaeggli, S., Kuhn, J., & Mickey, D. 2007b, ApJ, 670, 1521
Habbal, S. R., et al. 2010, ApJ, 708, 1650
Hudson, H. S., et al. 1999, ApJ, 513, L83
Janssen, P. J. 1868, C. R. Acad. Sci., 67, 838
Mackay, D. H., et al. 2010, Space Sci. Rev., 151, 333
Morgan, H., & Habbal, S. R. 2007, A&A, 465, L47
Morgan, H., & Habbal, S. R. 2010, ApJ, 710, 1
Morgan, H., Habbal, S. R., & Woo, R. 2006, Sol. Phys., 236, 263
Pasachoff, J. M., Rušin, V., Druckmüller, M., Aniol, P., Saniga, M., & Minarovjech, M. 2009, ApJ, 702, 1297
Pneuman, G. W. 1972, ApJ, 177, 793
Saito, K., & Tandberg-Hanssen, E. 1973, Sol. Phys., 31, 105
Scholl, I., & Habbal, S. R. 2008, Sol. Phys., 248, 425
Secchi, A. 1875, Le Soleil, vol. 1 (Paris: Gauthiers-Villars)
Secchi, A. 1877, Le Soleil, vol. 2 (Paris: Gauthiers-Villars)
Tandberg-Hanssen, E. 1995, The Nature of Solar Prominences (Dordrecht: Kluwer)
Vásquez, A. M., Frazin, R. A., & Kamalabadi, F. 2009, Sol. Phys., 256, 73
Yeates, A. R., Mackay, D. H., & van Ballegooijen, A. A. 2007, Sol. Phys., 245, 87
Yeates, A. R., Mackay, D. H., & van Ballegooijen, A. A. 2008, Sol. Phys., 247, 103